Inorg. Chem. **1994,** *33,* 3370–3381

Polymorphous Modifications of a Ni^{2+} Complex with Stable Nitroxide Involving Ni^{2+}–$O^•$–N Bonds. Quantum-Chemical Investigation of Exchange Interactions in Heterospin Systems

Victor I. Ovcharenko,[*,†] **Galina V. Romanenko,**[‡] **Vladimir N. Ikorskii,**[‡] **Ryza N. Musin,**[§] **and Renad Z. Sagdeev**[†]

International Tomography Center, Institute of Inorganic Chemistry, and Institute of Chemical Kinetics and Combustion, Siberian Branch of Russian Academy of Science, 630090 Novosibirsk, Russia

Received November 4, 1993[⊗]

It has been established that the Ni^{2+} bischelate with the deprotonanted enamine ketone derivative of stable 3-imidazoline nitroxide—bis[(1-(2,2,5,5-tetramethyl-1-oxyl-3-imidazolin-4-yl)-3′,3′,3′-trifluoro-1′-propenyl)-2′-oxy-*O′,N*³)]-nickel(II)—exists in the form of two polymorphous modifications (α-NiL_2 and β-NiL_2). We succeeded in obtaining each of these modifications in its pure state. X-ray data show both α-NiL_2 and β-NiL_2 to be layered polymeric structures. The polymeric structure is accounted for by the fact that each nickel ion coordinates $N^•$–O group oxygens of two adjacent molecules along with the enamineketone oxygens and nitrogens of its "own" ligands. However, the coordinated $N^•$–O groups in α-NiL_2 are in trans-position (Ni–$O^•$– 2.206(7) Å) while those in β-NiL_2 are in cis-position (Ni–$O^•$– 2.302(7) and 2.486(7) Å). The –$^•$O–Ni–$O^•$– angles are 180.0(2) and 85.1(2)° in α-NiL_2 and β-NiL_2, respectively. The structural difference of the polymorphous modifications determines the fundamental difference of their magnetic properties: in α-NiL_2, exchange interactions are antiferromagnetic ($J = -69.4\ cm^{-1}$), whereas β-NiL_2 contains both antiferromagnetic ($J \simeq -115\ cm^{-1}$) and ferromagnetic ($J \simeq 9.8\ cm^{-1}$) exchange clusters. A detailed quantum-chemical investigation of exchange interaction mechanisms in the ($N^•$–O–Ni^{2+}–$O^•$–N) heterospin exchange clusters and a critical analysis of available methods for calculating the exchange parameters *J* for heterospin systems have been performed in order to account for the fundamental difference in magnetic properties of α-NiL_2 and β-NiL_2 as well as the unexpected fact of ferromagnetic exchange in β-NiL_2 in the presence of direct contact of nonorthogonal magnetic orbitals. Both the conception of direct exchange interaction and the traditional molecular-orbital approach were found to be inadequate to describe the magnetic properties of α-NiL_2 and β-NiL_2 observed experimentally. The reason is that the molecular-orbital approach considers the configuration interactions (CI) of only two (ground and doubly excited) singlet configurations (2 × 2 CI) in the basis of frontier molecular orbitals (MO) and is meant primarily for the analysis of exchange interactions in metal complexes containing symmetrical exchange systems like {M}···{M}, where {M} is a fragment involving the paramagnetic metal ion. Of utmost importance for the correct estimation of exchange interaction values for heterospin complexes of transition metals with nonsymmetrical exchange systems like {M}···{L}, where {M} is the fragment containing the paramagnetic metal ion and {L} is the fragment containing the $O^•$–N group, is the incorporation of the third (singly excited) singlet configuration (3 × 3 CI) into the configuration interaction as well as to account for the contributions from the small delocalization of spin density in the directions $\{M\} \leftarrow \{L\}$ and $\{M\} \rightarrow \{L\}$. Crystal data: for α-NiL_2, orthorhombic *Pbca*, $a = 20.090(10)$ Å, $b = 10.685(4)$ Å, $c = 11.051(5)$ Å, $Z = 4$, $R = 0.0692$, $R_w = 0.0705$; for β-NiL_2, orthorhombic *Pbca*, $a = 19.921(1)$ Å, $b = 11.112(2)$ Å, $c = 21.549(3)$ Å, $Z = 8$, $R = 0.0476$, $R_w = 0.0476$.

Introduction

The last few years have seen an increased interest in the synthesis of molecular ferromagnets based on various heterospin systems such as coordination polymers containing different metals,[1–5] organometallic radical-ion compounds,[6–10] and the complexes of paramagnetic metal ions with stable nitroxides.[11–22] A considerable progress made in the synthesis of such ferro- and ferrimagnets is closely related to studying magnetostructural correlations in

---

[†] International Tomography Center, Siberian Branch of Russian Academy of Science.

[‡] Institute of Inorganic Chemistry, Siberian Branch of Russian Academy of Science.

[§] Institute of Chemical Kinetics and Combustion, Siberian Branch of Russian Academy of Science.

[⊗] Abstract published in *Advance ACS Abstracts,* June 1, 1994.

(1) Pei, Yu.; Verdaguer, M.; Kahn, O.; Sletten, J.; Renard, J.-P. *J. Am. Chem. Soc.* **1986**, *108*, 7428.

(2) Pei, Yu.; Verdaguer, M.; Kahn, O.; Sletten, J.; Renard, J.-P. *Inorg. Chem.* **1987**, *26*, 138.

(3) Kahn, O.; Pei, Yu.; Verdaguer, M.; Renard, J.-P.; Sletten, J. *J. Am. Chem. Soc.* **1988**, *110*, 782.

(4) Lloret, F.; Nakatani, K.; Journaux, Y.; Kahn, O.; Pei, Yu.; Renard, J.-P. *J. Chem. Soc., Chem. Commun.* **1988**, 642.

(5) Nakatani, K.; Carriat, J. Y.; Journaux, Y.; Kahn, O.; Lloret, F.; Renard, J.-P.; Pei, Yu.; Stetten, J.; Verdagner, M. *J. Am. Chem. Soc.* **1989**, *111*, 5739.

(6) Miller, J. S.; Zhang, J. H.; Reiff, W. M. *J. Am. Chem. Soc.* **1987**, *109*, 4584.

(7) Miller, J. S.; Calabrese, J. C.; Rommelmann, H.; Chittipeddi, S. R.; Zhang, J. H.; Reiff, W. M.; Epstein, A. J. *J. Am. Chem. Soc.* **1987**, *109*, 769.

(8) Miller, J. S.; Epstein, A. J.; Reiff, W. M. *Science* **1988**, *240*, 40.

(9) Miller, J. S.; Calabrese, J. C.; Epstein, A. J.; Bigelow, R. W.; Zhang, J. H.; Reiff, W. M. *J. Chem. Soc., Chem. Commun.* **1986**, 1026.

(10) Miller, J. S.; Epstein, A. J.; Reiff, W. M. *Acc. Chem. Res.* **1988**, *21*, 114.

(11) Caneschi, A.; Gatteschi, D.; Rey, P. *Prog. Inorg. Chem.* **1991**, *39*, 331.

(12) Caneschi, A.; Gatteschi, D.; Rey, P.; Sessoli, R. *Inorg. Chem.* **1988**, *27*, 1756.

(13) Caneschi, A.; Gatteschi, D.; Renard, J.-P.; Rey, P.; Sessoli, R. *Inorg. Chem.* **1989**, *28*, 1976.

(14) Caneschi, A.; Gatteschi, D.; Renard, J.-P.; Rey, P.; Sessoli, R. *Inorg. Chem.* **1989**, *28*, 3314.

(15) Caneschi, A.; Gatteschi, D.; Laugier, J.; Rey, P.; Sessoli, R. *Inorg. Chem.* **1988**, *27*, 1553.

(16) Caneschi, A.; Gatteschi, D.; Renard, J.-P.; Rey, P.; Sessoli, R. *J. Am. Chem. Soc.* **1989**, *111*, 785.

(17) Caneschi, A.; Gatteschi, D.; Sessoli, R.; Rey, P. *Acc. Chem. Res.* **1989**, *22*, 392.

(18) Ovcharenko, V. I.; Vostrikova, K. E.; Romanenko, G. V.; Ikorskii, V. N.; Podberezskaya, N. V.; Larionov, S. V. *Dokl. Akad. Nauk SSSR* **1989**, *306*, 115.

(19) Ovcharenko, V. I.; Vostrikova, K. E.; Ikorskii, V. N.; Larionov, S. V.; Sagdeev, R. Z. *Dokl. Akad. Nauk SSSR* **1989**, *306*, 660.

(20) Ovcharenko, V. I.; Ikorskii, V. N.; Vostrikova, K. E.; Burdukov, A. B.; Romanenko, G. V.; Pervukhina, N. V.; Podberezskaya, N. V. *Izv. Sib. Otd. Akad. Nauk SSSR, Ser. Khim. Nauk.* **1990**, *5*, 100.

(21) Ovcharenko, V. I.; Ikorskii, V. N.; Romanenko, G. V.; Reznikov, V. A.; Volodarskii, L. B. *Inorg. Chim. Acta* **1991**, *187(1)*, 67.

0020-1669/94/1333-3370$04.50/0

Chart 1

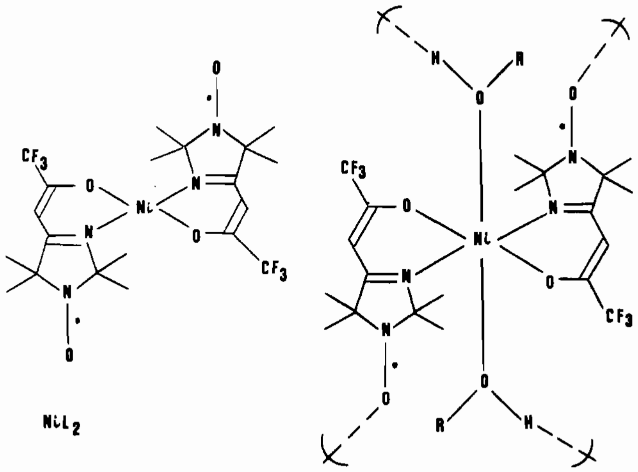

these systems. A knowledge of these correlations favors the purposive design of molecular ferromagnets.

Inasmuch as the present work is related to the synthesis of molecular ferromagnets based on the complexes of paramagnetic metal ions with stable nitroxides, it should be noted that among the compounds of this class of most interest at the moment are the complexes involving the derivatives of stable nitroxides of 2-imidazoline[11-17] or 3-imidazoline[18-22] heterocycles, which are polymeric in solid. Among the metal complexes with the derivatives of the stable 3-imidazoline nitroxide capable of magnetic phase transition to the ferromagnetic state at 5–7 K are the compounds of bis[(1-(2,2,5,5-tetramethyl-1-oxyl-3-imidazolin-4-yl)-(3′,3′,3′-trifluoro-1′-propenyl)-2′-oxy-*O′*,*N*³)]nickel(II) with alcohols of the composition $NiL_2(ROH)_2$, where R is the CH_3, C_2H_5, *n*-C_3H_7, *n*-C_4H_9, *n*-C_5H_{11}, or C_3H_5 group.[18-22] The layered polymeric structure is intrinsic in all these compounds due to the hydrogen bonding of OH groups of coordinated alcohol molecules and O atoms of N•–O groups of adjacent molecules (see Chart 1). One of the characteristic features of $NiL_2(ROH)_2$ complexes is the fact that, with the alcohol removed, they are transformed into NiL_2 which is unable to undergo the magnetic phase transitions to the ferromagnetic state. Since the crystal structure of $NiL_2(ROH)_2$ was available[18,20] and that of NiL_2 was unknown, the crucial question was open as to what distinctions between the crystal structures of $NiL_2(ROH)_2$ and NiL_2 made the magnetic properties of the compounds essentially different. It might be suggested that the removal of alcohol molecules results in the failure of the layered structure and formation of NiL_2 with a molecular structure. However, the previous investigation[23] of the magnetic properties of powdered NiL_2 samples has shown the presence of strong antiferromagnetic exchange interactions ($\simeq -100\ cm^{-1}$) in solid NiL_2, which is inconsistent with the assumption of the molecular crystal structure of NiL_2. Moreover, an attempt at theoretical description of the experimental dependence $\mu_{eff}(T)$ for NiL_2 by the (O•–N···Ni^{2+}···N•–O) exchange cluster model yielded a high *g*-factor for the metal ion, which is not characteristic of Ni^{2+}. This fact indicated that the given model was inadequate to describe the magnetic properties of NiL_2. At 4.2 K NiL_2 also exhibited a high residual magnetic moment ($\simeq 1\ \mu_B$), which contradicted the fact of strong antiferromagnetic exchange interaction between unpaired electrons in the (O•–N···Ni^{2+}···N•–O) exchange cluster for which, in this case, the ground state should correspond to the total spin $S = 0$. The unusual magnetic properties of NiL_2 and their essential difference from the magnetic properties of $NiL_2(ROH)_2$ impelled us to investigate solid NiL_2 in more detail.

The results of our study have shown that the "strange" magnetic properties of NiL_2 are determined by the nature of the complex, which is able to exist in two polymorphous modifications denoted as α-NiL_2 and β-NiL_2. The fundamental difference in magnetic properties of α-NiL_2 and β-NiL_2 called for a detailed quantum-chemical investigation of exchange interaction mechanisms for the (N•–O–Ni^{2+}–O•–N) heterospin exchange clusters and a critical analysis of available techniques for calculating J incorporated in the Heisenberg spin Hamiltonian $H = -2JS_AS_B$ since both the conception of direct exchange interaction[24-26] and the traditional molecular-orbital approach[27] were found to be inadequate to describe the magnetic properties of α-NIL_2 and β-NiL_2 observed experimentally. It should also be noted that researches dealing with the synthesis and investigation of metal complexes with stable nitroxides more and more often come up against the problem of the occurrence of the compounds in the form of several polymorphous modifications.[12,23,28,29] This, on the one hand, stands in the way of purposive design of molecular ferromagnets. However, on the other hand, studying the nitroxide–metal complexes which can exist in the form of several polymorphous modifications yields indubitably valuable information for the investigation of magnetostructural correlations. One of the parameters—the compound composition—remains in this case constant, which allows one to observe experimentally the effect of structural changes in the compound on its magnetic properties.

Experimental Section

NiL_2 was obtained from $NiL_2(C_2H_5OH)_2$ by heating at 60 °C in vacuo during 5–6 h. $NiL_2(C_2H_5OH)_2$ was synthesized as described elsewhere.[18] All solvents were commercial grade and were used as received.

Preparation of α-NiL_2. A 0.2-g sample of NiL_2 was refluxed in 50 mL of CH_2Cl_2 for an hour to prepare a saturated solution. (It should be noted that NiL_2 dissolves in hot CH_2Cl_2 rather slowly.) The solution was filtered, and 10 mL of heptane was added to the filtrate. The mixture was allowed to stay for 24 h at ambient temperature. Then, 10 mL of heptane was added to the mixture three times at intervals of 24 h; after that, the solution was kept at room temperature for 48 h. During all this time the cover did not fit snugly to the flask to allow the solvent to evaporate. As a result, in 144 h the volume of the solution reduced to 50–60 mL. Well-shaped needlelike yellow-brown α-NiL_2 crystals (0.08–0.09 g) were obtained. The crystals were collected on a frit, washed with heptane, and dried in air (mp 258–260 °C).

Adding hexane to the saturated NiL_2 solution, prepared as described above, in the ratio CH_2Cl_2:C_6H_{14} = 1:1.5 yields rather good α-NiL_2 crystals in 48–72 h. However the yield of crystals and their size in this case are usually less than those of the crystals obtained using heptane. The addition of hexane in a larger amount (CH_2Cl_2:C_6H_{14} = 1:2–1:3) results in faster and practically quantitative crystallization of NiL_2. However, in this case, along with α-NiL_2, whose formation was predominant, β-NiL_2 was also crystallized. Since β-NiL_2 crystals essentially differ from α-NiL_2 crystals in shape and color, α-NiL_2 can be separated from β-NiL_2 mechanically. All α-NiL_2 samples, irrespective of the method of preparation, exhibited the same physical and chemical characteristics.

Preparation of β-NiL_2. β-NiL_2 crystals in the form of light green square plates were grown from a solution of the complex in pure CH_2Cl_2. The latter gradually evaporated in 24 h at ambient temperature. β-NiL_2 can also be isolated mechanically from the mixture of α-NiL_2 and β-NiL_2 crystals formed as described above in the recrystallization of NiL_2 from a CH_2Cl_2–hexane mixture with excessive hexane content. Irrespective of the preparation method, all β-NiL_2 samples showed the same physical and chemical characteristics. When heated up to 170–190 °C, β-NiL_2 crystals transformed into α-NiL_2, cracked, and changed their color from

---

(22) Vostrikova, K. E.; Ovcharenko, V. I.; Romanenko, G. V.; Ikorskii, V. N.; Podberezskaya, N. V.; Reznikov, V. A.; Volodarskii, L. B. *Zh. Neorg. Khim.* **1992**, *37*, 1755.

(23) Ikorskii, V. N.; Ovcharenko, V. I. *Zh. Neorg. Khim.* **1990**, *35*, 2093.

(24) McWeeny, R.; Yonezawa, F. *J. Chem. Phys.* **1965**, *43*, S120.

(25) Dackre, P. D.; McWeeny, R. *Proc. R. Soc. London* **1970**, *A317*, 435.

(26) Schastnev, P. V.; Salikhov, K. M. *Theor. Eksper. Khim.* **1973**, *9*, 291.

(27) Hay, P. J.; Thibeault, J. C.; Hoffmann, R. *J. Am. Chem. Soc.* **1975**, *97*, 4884.

(28) Ikorskii, V. N.; Ovcharenko, V. I.; Vostrikova, K. E.; Pervukhina, N. V.; Podberezskaya, N. V. *Zh. Neorg. Khim.* **1992**, *37*, 1177.

(29) Caneschi, A.; Gatteschi, D.; Laugier, J.; Rey, P.; Sessoli, R.; Zanchini, C. *J. Am. Chem. Soc.* **1988**, *110*, 2795.

Table 1. Crystallographic Data for α-NiL_2 and β-NiL_2

	α-NiL_2	β-NiL_2
chem formula	$C_{20}H_{26}F_6N_4NiO_4$	$C_{20}H_{26}F_6N_4NiO_4$
a, Å	20.090(10)	19.921(2)
b, Å	10.685(4)	11.112(1)
c, Å	11.051(5)	21.549(3)
V, Å^3	2372(2)	4769.9(9)
Z	4	8
fw	559.21	559.21
space group	*Pbca*	*Pbca*
T, K	298	298
λ, Å	1.541 78	0.710 69
ρ_{calcd}, g cm^{-3}	1.57	1.56
μ, cm^{-1}	17.77	8.9
$R(F_o)^a$	0.0692	0.046
$R_w(F_o)^b$	0.0705	0.046

[a] $R = \sum||F_o| - |F_c||/\sum|F_o|$. [b] $R_w = [\sum w(|F_o| - |F_c|)^2/\sum|F_o|^2]^{1/2}$.

Table 2. Atom Coordinates ($\times 10^4$) and Temperature Factors (Å $\times$ 10^3) for α-NiL_2

atom	x	y	z	U_{eq}^a
Ni	0000	5000	5000	21(1)
O(1)	954(3)	4603(5)	4810(5)	25(3)
N(1)	236(3)	6130(6)	6493(5)	18(4)
C(1)	1420(4)	4821(8)	5564(7)	23(5)
C(01)	2075(5)	4190(10)	5242(8)	38(6)
F(1)	2038(4)	2992(7)	5300(10)	117(7)
F(2)	2230(3)	4380(10)	4112(6)	108(6)
F(3)	2575(3)	4533(8)	5881(6)	92(5)
C(2)	1397(4)	5510(10)	6597(7)	28(5)
C(3)	826(4)	6159(8)	6983(7)	22(5)
C(4)	895(4)	7039(8)	8062(7)	26(5)
C(41)	1013(7)	6370(10)	9240(10)	48(8)
C(42)	1425(6)	8040(10)	7840(10)	41(7)
N(11)	229(3)	7587(7)	8037(6)	27(4)
O(11)	4(3)	8348(6)	8803(6)	48(4)
C(5)	–228(4)	6954(8)	7149(7)	26(5)
C(51)	–742(5)	6250(10)	7860(10)	31(6)
C(52)	–537(5)	7960(10)	6350(10)	33(6)

[a] $U_{eq} = {}^1/_3(U_{11} + U_{22} + U_{33})$.

light green to brown. Analytical data for α-NiL_2 and β-NiL_2 corresponded well to the composition of $NiC_{20}H_{26}N_4O_4F_6$.

Crystal Structure Determination. Reflections were collected with automated diffractometers Syntex $P2_1$ (Cu Kα, graphite monochromator) for α-NiL_2 and Enraf Nonius CAD-4 (Mo Kα, graphite monochromator) for β-NiL_2. Parameters of unit cells were refined by 20 patterns in the range $20° < 2\theta < 30°$ (α-NiL_2) and by 15 patterns at $18° < 2\theta < 20°$ for β-NiL_2. Data were collected in a $\theta/2\theta$ scan with variable rate $V_{min} = 7°$/min, $2\theta_{max} = 110°$ (α-NiL_2) and in a $\theta/2\theta$ scan up to $2\theta = 50°$ (β-NiL_2). The intensities of three standard reflections were measured for every 100 reflections for α-NIL_2 and for every 42 reflections for β-NiL_2. The measured intensities were corrected for Lorentz and polarization factors; absorption corrections were applied by ψ-scan data for α-NiL_2 and using the DIFABS[30] program for β-NiL_2. The structures were solved by a direct method using the SHELXS-86[31] program. After a few cycles of refinement (full-matrix least-squares technique) of all non-hydrogen atoms in terms of anisotropic approximation in the difference Fourier syntheses all H atoms were localized and, then, incorporated in the refinement in isotropic approximation. Final values of R factors were given above together with other crystallographic data. The structure refinement was carried out using the YANX[32] software on an EC-1037 computer.

Crystallographic data and final atomic coordinates with thermal parameters for α-NiL_2 and β-NiL_2 are given in Tables 1–3, respectively.

Table 3. Atom Coordinates ($\times 10^4$) and Temperature Factors (Å $\times$ 10^3) for b-NiL_2

atom	x	y	z	U_{eq}^a
Ni	8791	1925(1)	3092	7.7(4)
O(1)	9301(2)	2030(5)	3869(2)	29(3)
N(1)	8106(3)	794(5)	3505(3)	24(3)
C(1)	9128(4)	1583(7)	4401(3)	31(4)
C(01)	9604(5)	194(1)	4914(4)	46(6)
F(1)	9624(4)	3122(6)	4994(3)	90(5)
F(2)	10237(3)	1622(7)	4776(3)	85(5)
F(3)	9462(3)	1458(6)	5456(2)	77(4)
C(2)	8591(4)	887(8)	4537(4)	38(5)
C(3)	8120(4)	473(7)	4083(4)	33(5)
C(4)	7599(4)	–439(7)	4264(4)	36(5)
C(41)	7925(6)	–1610(10)	4508(5)	49(6)
C(42)	7072(6)	40(10)	4726(5)	53(7)
N(11)	7301(3)	–642(6)	3658(3)	37(4)
O(11)	6804(3)	–1359(5)	3588(3)	50(4)
C(5)	7545(4)	191(7)	3174(4)	32(4)
C(51)	6995(5)	1100(10)	3011(6)	50(6)
C(52)	7781(5)	–509(8)	2621(4)	40(5)
O(2)	8273(3)	2355(5)	2353(2)	29(3)
N(2)	9364(3)	720(5)	2596(3)	27(4)
C(6)	8417(4)	2092(6)	1794(3)	23(4)
C(06)	7980(4)	2670(8)	1313(4)	41(5)
F(4)	8045(3)	3865(5)	1307(3)	72(4)
F(5)	8074(3)	2300(5)	738(2)	67(4)
F(6)	7329(3)	2489(7)	1439(3)	80(4)
C(7)	8899(4)	1323(7)	1585(4)	29(4)
C(8)	9331(4)	638(7)	1990(4)	31(4)
C(9)	9766(4)	–327(7)	1712(3)	28(4)
C(91)	9341(5)	1320(10)	1411(5)	47(6)
C(92)	10290(5)	200(10)	1262(5)	45(6)
N(21)	10084(3)	–778(6)	2276(3)	32(4)
O(21)	10509(3)	–1626(5)	2312(3)	55(4)
C(10)	9865(4)	–130(7)	2837(4)	31(5)
C(101)	10451(5)	530(10)	3124(6)	47(6)
C(102)	9536(6)	–1000(10)	3289(5)	52(7)

[a] $U_{eq} = {}^1/_3(U_{11} + U_{22} + U_{33})$.

Magnetic Susceptibility Measurements. The magnetic susceptibilities (χ_M) of samples were measured by the Faraday method in the temperature range 4.2–463 K and at the magnetic fields up to 10.9 kOe. The effective magnetic moment was calculated by the formula $\mu_{eff} = (8\chi_M T)^{1/2}$. In the calculations of χ_M we used the following values of diamagnetic contribution and temperature-independent paramagnetism: 296×10^{-6} and 190×10^{-6} cm^3/mol, respectively. The optimal J, $J'z'$, and g_{Ni} values were obtained by minimization of the $\sum_i[\mu_{eff}^{calcd}(T_i) - \mu_{eff}^{measd}(T_i)]^2$ sum.

Results and Discussion

To find out the possibility of the existence of NiL_2 in a few polymorphous modifications we studied the products of its crystallization from different solvents such as hexane, heptane, chloroform, methylene chloride, carbon tetrachloride, and benzene (and their mixtures) whose molecules exhibit no pronounced donor ability. Otherwise, due to the high accepting ability of the central atom, the resulting crystals are mixed-ligand complexes with solvent molecules[20] (like those mentioned above, e.g., $NiL_2(ROH)_2$). It has been observed that the most well-shaped and large NiL_2 single crystals suitable for X-ray analysis are formed from methylene chloride and from its mixtures with hexane or heptane. The crystallization of NiL_2 from methylene chloride or from a mixture of methylene chloride with hexane and heptane can be carried out (see Experimental Section) so that the solid will involve NiL_2 crystals of a certain modification. If both α-NiL_2 and β-NiL_2 are crystallized simultaneously, one can readily separate these modifications of NiL_2 mechanically. It should also be noted that in all our experiments we saw the formation of either one of the modifications, α-NiL_2 and β-NiL_2, or their mixture. No other modifications of NiL_2 were observed. The α-NiL_2 and β-NiL_2 crystals differ in shape and color. They show essentially different diffraction patterns and IR spectra, which allows their easy identification. It is noteworthy that the experimental diffraction patterns of α-NiL_2 and β-NiL_2 powders coincide with those theoretically calculated from data of experiments with single crystals. Heating of β-NiL_2 up to 160–185 °C leads to its complete transformation into α-NiL_2, with the color

---

(30) Walker, N.; Stewart, D. *Acta Crystallogr.* **1983**, *A39*, 158.
(31) Sheldrick, G. M. *Acta Crystallogr.* **1990**, *A46*, 467.
(32) Gerr, R. G.; Yanowskii, A. I.; Struchkov, Yu. T. *Kristallografiya* **1983**, *28*, 1029.

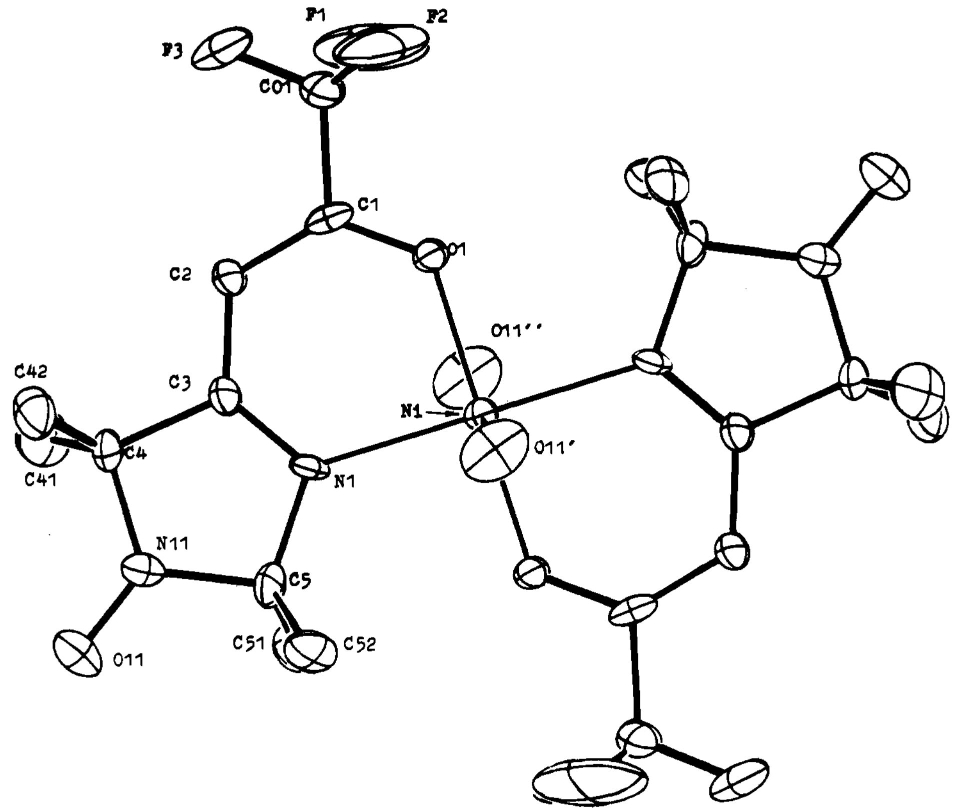

Figure 1. ORTEP drawing of the Ni^{2+} environment in the structure of α-NiL$_2$ with the numbering scheme used in the Tables. Ellipsoids are shown at 35% probability.

changing from light green, typical of β-NiL$_2$ crystals, to brown, inherent in α-NiL$_2$. It is rather interesting to observe this process in sufficiently large and well-shaped β-NiL$_2$ crystals with a microscope. The color changes layer-by-layer. One can see sequential "run" of overlapping layers. The light green color of crystals gradually changes to brown. The darkening of the crystals is also due to their cracking during the transformation of β-NiL$_2$ to α-NiL$_2$, which, thus, is not topochemical. But the complex does not decompose since the decomposition temperature for α-NiL$_2$ is above 200 °C.

Crystal Structure. The environment of the central atom in α-NiL$_2$ is a slightly distorted centrosymmetric octahedron (shown in Figure 1). There are O and N atoms of the enamineketone groups of both L in the equatorial plane. The axial positions are occupied by O atoms of N$^\bullet$–O groups of adjacent molecules. The distances Ni–O, Ni–N, and Ni–O$^\bullet$– are 1.974(5), 2.098(6), and 2.206(7) Å, respectively; the ONiN angle in the chelate ring equals 89.3(2)°. In β-NiL$_2$ the environment of the Ni atom is also octahedral, but the coordinated O atoms of N$^\bullet$–O groups of adjacent molecules are in cis-position (Figure 2). The average values of Ni–O and Ni–N distances and ONiN angles in the chelate rings of β-NiL$_2$ are practically the same as those in α-NiL$_2$: 1.960(5), 2.058(6) Å, 91.2(2)°. The Ni–O$^\bullet$– distances are much longer: 2.302(7) and 2.486(7) Å. The –$^\bullet$ONiO$^\bullet$– angle is 85.1(2)°, the –$^\bullet$O$\cdots$O$^\bullet$– distance in the coordination polyhedron of β-NiL$_2$ is 3.241(9) Å.

The ligand geometries in α-NiL$_2$ and β-NiL$_2$ are practically the same and show good agreement with data on the complexes of other metals with L.[33,34] The chelate metallocycles are practically planar, as are the imidazoline heterocycles (including the N$^\bullet$–O group oxygen). The maximum deviation of atoms from the rms planes are equal to or less than 0.09 Å. The angles between the metallocycle and imidazoline heterocycle planes are no more than 8°; i.e., ligands in the complexes are bonded along the common bond of the C–N cycles. The centrosymmetric octahedral environment of the Ni atom in α-NiL$_2$ determines the angle between the chelate cycle planes, 180°; in β-NiL$_2$ this angle

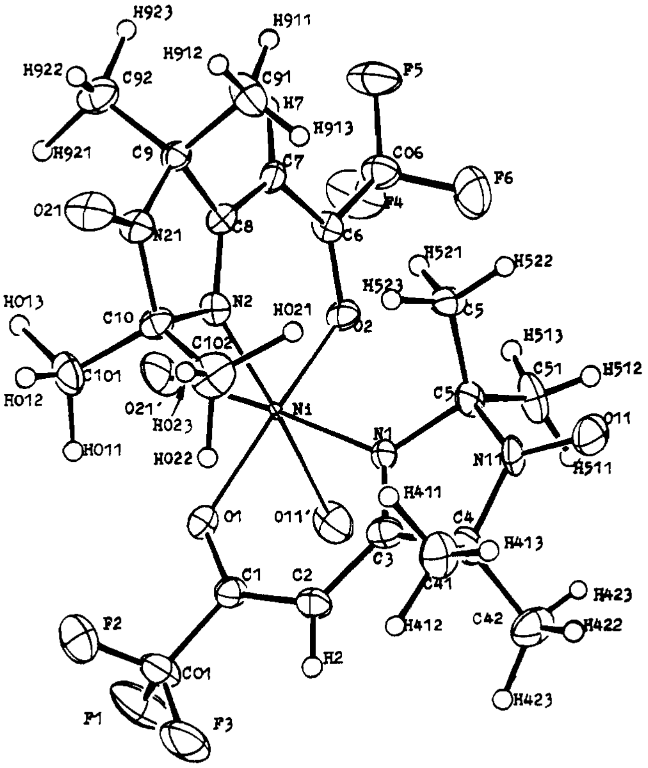

Figure 2. ORTEP drawing of the Ni^{2+} environment in the structure of β-NiL$_2$ with numbering scheme used in the Tables. Ellipsoids are shown at the 35% probability.

---

(33) Pervukhina, N. V.; Ikorskii, V. N.; Podberezskaya, N. V.; Nikitin, P. S.; Helman, A. B.; Ovcharenko, V. I.; Larionov, S. V.; Bakakin, V. V. *Zh. Struckt. Khim.* **1986**, *27*, N4, 61.

(34) Romanenko, G. V.; Podberezskaya, N. V.; Ovcharenko, V. I. *Zh. Neorg. Khim.* **1992**, *37*, 1525.

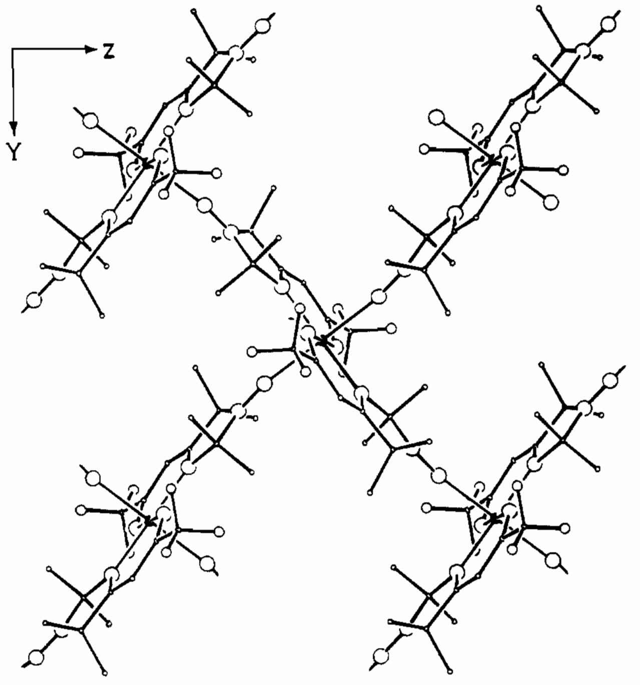

Figure 3. Projection of the polymeric layer in the structure of α-NiL_2 onto the (100) plane.

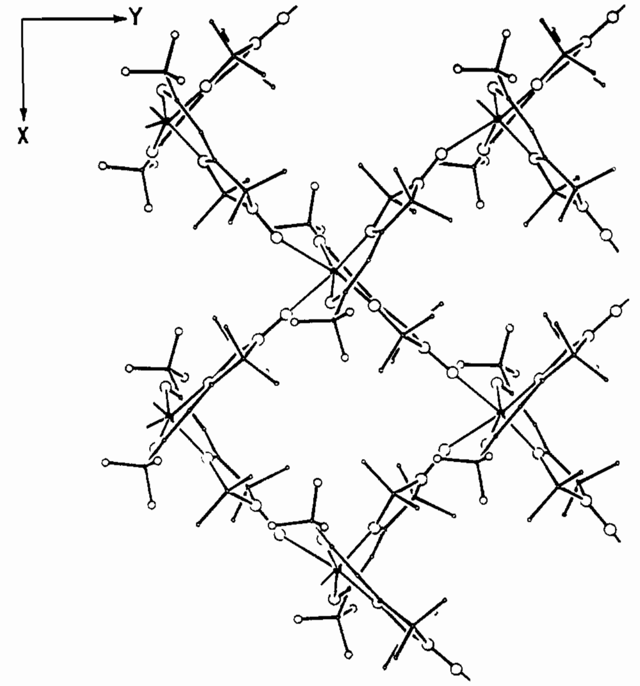

Figure 4. Projection of the polymeric layer in the structure of β-NiL_2 onto the (001) plane.

is 78.4°. The N•–O bond lengths in the nitroxyl groups of both the complexes lies within the range 1.257(9)–1.281(9) Å, which is typical of nitroxyl groups;[35] the Ni–O•–N angles are within 153.7(5)–157.2(6)°. The distances Ni···•O in NiL_2 fragments range between 5.487(6) and 5.519(6) Å. The coordination of nitroxide groups by metal atom of the adjacent molecule determines the layered polymeric structure of the complexes. Figures 3 and 4 show the projections of polymeric layers in α-NiL_2 and β-NiL_2 structures. In both structures, the van der Waals interactions between atoms of polymeric layers are weak. The shortest interlayer distances F···F are 3.149(8) and 3.774(10) Å in β-NiL_2 and α-NiL_2, respectively. It should be noted that in α-NiL_2, paramagnetic centers (involving Ni^{2+} and O atoms of N•–O groups) lie practically in the same plane (the deviation is no more than 0.01 Å), while in β-NiL_2, due to crimped layers, the distances between the planes involving paramagnetic centers are 4.70 Å. Figure 5 shows schematically the disposition of paramagnetic centers in the polymeric layer of β-NiL_2. The values of bond lengths and angles of β-NiL_2 and α-NiL_2, most important for the following discussion, are listed in Table 4.

Magnetic Properties. Figure 6 shows a plot for $\mu_{eff}(T)$ for α-NiL_2 in the range 4.2–463 K. The decrease in μ_{eff} with decreasing temperature for α-NiL_2 is indicative of significant antiferromagnetic interactions between unpaired electrons of paramagnetic centers with the ground state $S = 0$. Obviously, such a strong antiferromagnetic exchange interaction can be realized only in a centrocymmetric exchange cluster (N•–O–Ni^{2+}–O•–N) since in the (O•–N···Ni^{2+}···N•–O) clusters for Ni^{2+} complexes with the derivatives of stable 3-imidazoline nitroxide, which have the molecular structure,[20,36] exchange interactions are usually no more than 10–15 cm^{-1}. Experimental data were fitted in terms of an exchange cluster consisting of Ni^{2+} and two nitroxides.[37] The spin Hamiltonian for such a cluster at a magnetic field $\mathcal{H}$ is as follows:

$$\hat{H} = -2J\hat{s}\hat{s}' - D\hat{s}_z^{\,2} - \beta(g\hat{s}_z + g'\hat{s}'_z)\mathcal{H} - 2J'z'\hat{S}_z\langle S_z\rangle \quad (1)$$

Here J and J' are the energy of exchange interaction between Ni^{2+} and radical and the intercluster exchange interaction energy, respectively; z' is the number of close neighbors of the clusters; $\hat{s}$ is the Ni^{2+} spin operator; $\hat{s}' = s_1 + s_2$ is the operator of the total spin of two radicals; D is the splitting parameter of Ni^{2+} at zero field; g and g' are the g factors of Ni^{2+} and the N•–O group of the radical (the g factor of the nitroxyl group was taken as 2); β is the Borh magneton; $\hat{S} = \hat{s} + \hat{s}'$ is the operator of the total cluster spin; $\langle S_z\rangle$ is the average projection of cluster spin onto the z axis. Specific formulas for magnetic susceptibility and of μ_{eff} for Hamiltonian (1) are given elsewhere.[37] Using these formulas we have obtained the optimum parameters of spin Hamiltonian (1) for α-NiL_2: $g = 2.00 \pm 0.02$, $J = -69.4 \pm 0.8$ cm^{-1}, and $D = -0.3 \pm 0.2$ cm^{-1}, $J'z' = 0.01 \pm 0.05$ cm^{-1}. (The solid line in Figure 6 is the corresponding optimal theoretical curve for 0–463 K). The low g factor of Ni^{2+} can be accounted for by two factors. First, this model implies much larger energy of intracluster exchange interaction as compared to the energies of other exchange interactions, which is not met in this particular case since along with the main exchange clusters (N•–O–Ni^{2+}–O•–N), the system involves the "intramolecular" exchange clusters (O•–N···Ni^{2+}···N•–O). Second, for α-NiL_2, a small residual moment is observed at 4.2 K ($\simeq 0.3$ μ_B), which currently cannot be accounted for. However, for the following discussion of most importance is only the fact that exchange interactions in the (N•–O–Ni^{2+}–O•–N) clusters are predominant and antiferromagnetic.

As can be seen from Figure 6, the temperature dependence $\mu_{eff}(T)$ for β-NiL_2 is rather complicated. It indicates the presence of both antiferromagnetic and ferromagnetic exchange interactions in β-NiL_2. The behavior of this function may be accounted for assuming the nonequivalent interactions of Ni^{2+} with two radicals, i.e., assuming that the exchange interaction between Ni^{2+} and one of the radicals is antiferromagnetic ($J_1 < 0$), the interaction of this ion with the other radical being ferromagnetic ($J_2 > 0$), and $|J_1| > J_2$. Such a model allows us to fit the function $\mu_{eff}(T)$ for β-NiL_2 separately for high- and low-temperature regions. In data fitting for the high-temperature region ($T > 150$), the following approximation is used: the exchange cluster involves Ni^{2+} and one radical. The interaction of the second

---

[35] Shibaeva, R. P. *Zh. Strukt. Khim.* **1975**, *16*, N2, 330.

[36] Ovcharenko, V. I.; Helman, A. B.; Ikorskii, V. N. *Zh. Strukt. Khim.* **1989**, *30*, N5, 142.

[37] Helman, A. B.; Ikorskii, V. N. *Koord. Khim.* **1988**, *14*, 491.

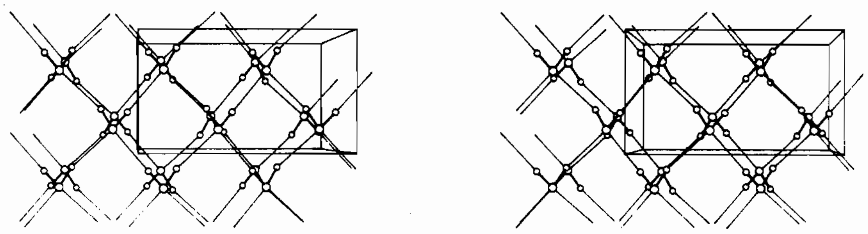

Figure 5. Stereo ORTEP drawing of β-NiL_2 showing the packing of paramagnetic center (Ni^{2+} ions (◯)) and oxygen atoms of $N^\bullet$–O groups (○)) in the polymeric layers of β-NiL_2.

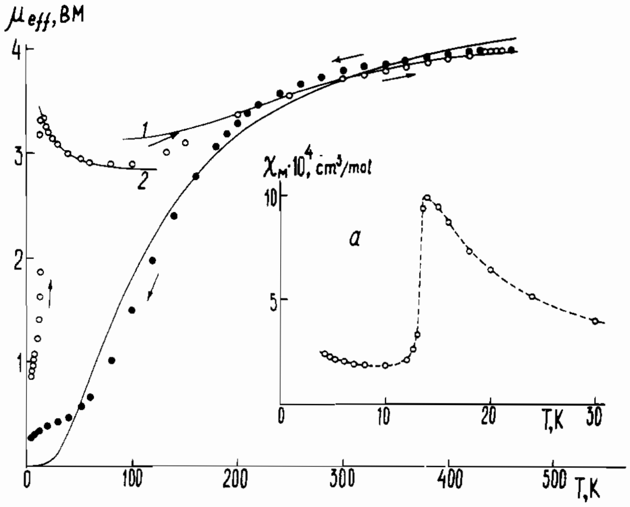

Figure 6. Experimental dependences $\mu_{eff}(T)$ for α-NiL_2 (●) and β-NiL_2 (○). The solid line represents the optimal theoretical curve obtained by the model of the isolated exchange cluster ($N^\bullet$–O–Ni^{2+}–$O^\bullet$–N). The solid lines 1 and 2 are the theoretical curves obtained as described in the text. Inset: plot of χ versus T over the range 4.2–30 K for β-NiL_2, indicative of the antiferromagnetic ordering.

Table 4. Selected Bond Lengths (Å) and Bond Angles (deg) for α-NiL_2 and β-NiL_2

	α-NiL_2	β-NiL_2
	Bond Lengths	
Ni–O(1)	1.974(5)	1.963(5)
Ni–N(1)	2.098(6)	2.057(6)
Ni–O(11′)	2.206(7)	2.486(7)
Ni–O(2)		1.957(5)
Ni–N(2)		2.059(6)
Ni–O(21′)		2.302(7)
N(11)–O(11)	1.257(9)	1.281(9)
N(21)–O(21)		1.269(9)
	Bond Angles	
O(1)NiN(1)	89.3(2)	90.6(2)
O(2)NiN(2)		91.7(2)
NiO(11′)N(11′)	157.2(6)	153.7(5)
NiO(21′)N(21′)		154.2(5)

radical with this exchange cluster is considered weak. In fact, this weak interaction is taken into account in the parameter of intercluster exchange interaction $J'z'$. Data fitting in terms of this approximation for $T > 150$ K yields the following optimal parameters: $g = 2.66 \pm 0.02$, $J = -115 \pm 1$ cm^{-1}, $D = -7.3 \pm 0.2$ cm^{-1}, $J'z' = 0.01 \pm 0.05$ cm^{-1}. (The theoretical curve corresponding to these parameters is represented by solid line 1 in Figure 6.) Certainly, this model is not exact, which is seen from the overestimated value of g. However, using this model, we managed to estimate the value of J (−115 cm^{-1}). This value suggests that at $T < 100$ K we have almost complete coupling of one of the unpaired Ni^{2+} electrons and the unpaired electron of one of the radicals. This simplifies determining the energy of the weaker exchange interaction of Ni^{2+} and the second radical. The calculation of magnetic properties of β-NiL_2 at low temperature reduces to the calculation of the (Cu–$O^\bullet$–N) cluster for which an exact solution is available in terms of the isotropic spin Hamiltonian[36]

$$\hat{H} = -2J\hat{s}\hat{s}'_1 - \beta(g\hat{s}_z + g'\hat{s}_{1z})\mathcal{H} - 2J'z'\hat{S}_z\langle S_z\rangle$$

where $\hat{s}$ and $\hat{s}_1$ are the operators of metal ion spin and organic radicals, respectively. The other parameters are the same as in Hamiltonian (1). The magnetic susceptibility per one exchange cluster (Cu–$O^\bullet$–N) including the intercluster interaction is as follows[36]

$$\chi = \chi_{\mu,\mathcal{H}} + 2J'z'\frac{\chi_{\mu,\mathcal{H}}\chi_{s,\mathcal{H}}}{1 - 2J'z'\chi_{s,\mathcal{H}_m}} \qquad (2)$$

where $\chi_{\mu,\mathcal{H}}$, $\chi_{\mu,\mathcal{H}_m}$, $\chi_{s,\mathcal{H}}$, and $\chi_{s,\mathcal{H}_m}$ are the generalized susceptibilities which determine the response of the system (magnetic moment or spin) to corresponding perturbation (external field $\mathcal{H}$ or molecular field $\mathcal{H}_m$). The first term of eq 2 is the magnetic susceptibility of the (Cu–$O^\bullet$–N) exchange cluster in the absence of the intercluster interaction $J'z'$ and is determined by the following expression:

$$\chi_{\mu,\mathcal{H}} = \frac{\beta^2}{2kT}\frac{(g + g')^2 + \frac{kT}{2J}(g - g')^2(1 - e^{-2J/kT})}{3 + e^{-2J/kT}}$$

The other terms of the above formula are represented as follows:

$$\chi_{\mu,\mathcal{H}_m} = \chi_{s,\mathcal{H}} = \frac{\beta}{kT}\frac{g + g'}{3 + e^{-2J/kT}}$$

$$\chi_{s,\mathcal{H}_m} = \frac{2}{kT}\frac{1}{3 + e^{-2J/kT}}$$

The optimization of experimental data according to the (Cu–$O^\bullet$–N) exchange cluster model at $T = 15$–60 K gives the following parameters: $g = 2.43 \pm 0.02$; $J = 9.8 \pm 0.5$ cm^{-1}; $J'z' = 1.4 \pm 0.1$ cm^{-1} (curve 2 in Figure 6).

It should be noted that the approach proposed by Malinovskaya and Schastnev[53] allows the optimization of the experimental dependence $\mu_{eff}(T)$ for β-NiL_2 within 15–439 K with simultaneous account of two different energies of the exchange interactions of Ni^{2+} with each of the radicals (J_1 and J_2). In this case, the optimal fitting parameters are the following: $g_{Ni} = 2.29$, $J_1 = -154.0$ cm^{-1}, $J_2 = 18.2$ cm^{-1}, $D = 1.2$ cm^{-1}, and $J'z' = 2.7$ cm^{-1}. A comparison of these J values (−154.0 and 18.2 cm^{-1}) with those obtained by fitting of the experimental dependence $\mu_{eff}(T)$ for β-NiL_2 separately for the temperature regions 15–60 K and >150 K (−115 and 9.8 cm^{-1}) has shown that the J value lower in magnitude is positive regardless of the method of experimental data fitting.

The fact that exchange interactions between unpaired electrons of paramagnetic centers in β-NiL_2 are essentially different from those in α-NiL_2 is supported by the $\chi^{-1}(T)$ functions for both the

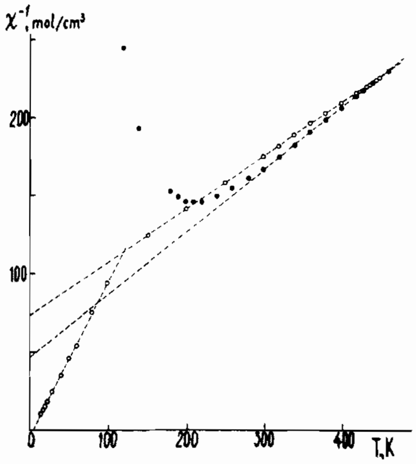

Figure 7. Experimental dependences χ^{-1} versus T for α-NiL$_2$ (●) and β-NiL$_2$ (○).

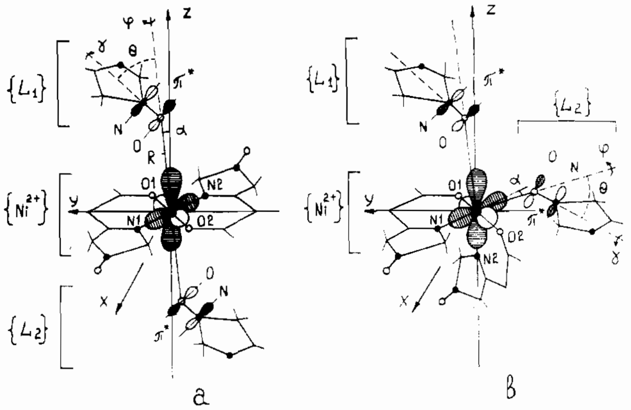

Figure 8. Schematic representations of the structures, main geometrical parameters, and magnetic orbitals of the exchange systems $\{L_2\}\cdots\{Ni^{2+}\}\cdots\{L_1\}$ for α-NiL$_2$ (a) and β-NiL$_2$ (b). Here R is the Ni–O(L$_p$) distance; θ is the angle between the Ni–O(L$_p$) and O(L$_p$)–N(L$_p$) bonds; φ is the angle of $\{L_p\}$ rotation about the Ni–O(L$_p$) bond and is equal to the angle between the O(L$_1$)–N(L$_1$) bond projection onto the N(1)–Ni–O(1) plane and the Ni–N(1) bond (for α-NiL$_2$ and β-NiL$_2$) or to the angle between the projection of the O(L$_2$)–N(L$_2$) bond onto the N(2)–Ni–O(2) plane and Ni–O(2) bond (for β-NiL$_2$); γ is the dihedral angle between the Ni–O(L$_p$)–N(L$_p$) plane and the plane of the nitroxide $\{L_p\}$; angle α characterizes the deviation of the Ni–O(L$_p$) bond from perpendicular to the N(1)–Ni–O(1) plane (for α-NiL$_2$ and β-NiL$_2$) or to the N(2)–Ni–O(2) plane (for β-NiL$_2$). The values of R, θ, φ, γ, and α for α-NiL$_2$ and β-NiL$_2$ are listed in Table 5.

polymorphs in Figure 7. The line for β-NiL$_2$ exhibits two linear sections which obey the Curie–Weiss law $\chi_M = c/(T - \Theta)$:

$$\text{(line 1) } T > 150 \text{ K} \quad c = 2.8; \Theta = -202 \text{ K}$$

$$\text{(line 2) } T = 15\text{–}60 \text{ K} \quad c = 1.0; \Theta = 4.6 \text{ K}$$

The two Weiss constants Θ, different in both value and sign, are unambiguously indicative of two essentially different exchange interactions in solid β-NiL$_2$.

The assumption of nonequivalent exchange interactions of Ni^{2+} with each radical, employed in the fitting of the experimental function $\mu_{eff}(T)$ for β-NiL$_2$, was not accidental. This assumption was borne out when, searching for the reasons for the occurrence of two essentially different types of exchange clusters, we could not disregard the geometrical differences in the Ni^{2+}–O$^•$–N fragments of β-NiL$_2$ (the difference is already seen from the bond lengths: for two cis-coordinated nitroxy groups the Ni–O$^•$– distances are 2.302 and 2.486 Å). This suggested that exchange interactions in β-NiL$_2$ were different in value and in sign namely in the (Ni^{2+}–O$^•$–N) exchange clusters. For β-NiL$_2$, the localization of strong antiferromagnetic exchange (on the order of −115 cm^{-1}) in the (Ni^{2+}–O$^•$–N) cluster was beyond question due to the reasons similar to those for α-NiL$_2$. However, we could not ascribe definitively the ferromagnetic exchange interactions to another (Ni^{2+}–O$^•$–N) cluster since the exchange value ($\simeq$10 cm^{-1}) in this case is comparable with that in the (Ni$^{2+}\cdots$N$^•$–O) clusters in Ni^{2+} complexes with 3-imidazoline nitroxide derivatives which show molecular structure and whose solids have no Ni–O$^•$–N coordinations. The elucidation of the possibility of ferromagnetic exchange in the (Ni^{2+}–O$^•$–N) exchange cluster required a quantum-chemical investigation of exchange interactions in this cluster.

Before proceeding to the quantum-chemical analysis of exchange interactions in α-NiL$_2$ and β-NiL$_2$, we shall note that Figure 6 (insert) presents one more important result. At $T < 14$ K, the χ_M value for β-NiL$_2$ dramatically decreases. This is due to the three-dimensional antiferromagnetic ordering of magnetic moments of the complex at $T_N = 14$ K. In addition, arrows along the experimental $\mu_{eff}(T)$ curves show changes in μ_{eff} for β-NiL$_2$ in going from low temperatures of the sample up to 463 K. At this temperature β-NiL$_2$ transforms completely to α-NiL$_2$ and further cooling leads to the $\mu_{eff}(T)$ values equal to those for α-NiL$_2$. Since the polymorphous transformation in this case is irreversible, repeated cool–heat cycles result in $\mu_{eff}(T)$ values intrinsic only in α-NiL$_2$. The α-NiL$_2$ complex can be transformed back to β-NiL$_2$ only via crystallization from CH$_2$Cl$_2$ by the procedure described in the Experimental Section. However, it should be emphasized once more that well-shaped β-NiL$_2$ crystals appear from the CH$_2$Cl$_2$ solution only when the solvent is completely evaporated in 12–24 h. At the lower rate of evaporation (a few days), both β-NiL$_2$ and α-NiL$_2$ crystals are formed which should be separated mechanically. If one does not need well-shaped β-NiL$_2$ crystals, it suffices to dissolve α-NiL$_2$ in hot CH$_2$Cl$_2$ and to evaporate the solution fast to dryness. The dry residual in this case is fine-grained pure β-NiL$_2$. These data show that of the two polymorphous modifications under study α-NiL$_2$ exhibits the higher thermodynamic stability.

Quantum-Chemical Analysis. A number of complexes of bis(hexafluoroacetylacetonato)nickel(II) with nitroxides (or nitronyl nitroxides) have been previously described for which the coordination of N$^•$–O groups by Ni^{2+} ion has been reliably supported by X-ray data.[38-40] Thus, α-NiL$_2$ and β-NiL$_2$ simply extend the number of Ni^{2+}–nitroxide complexes with the Ni–O$^•$–N coordination. However, in all complexes of this type, including α-NiL$_2$, the strong antiferromagnetic exchange interactions are observed in the (Ni^{2+}–O$^•$–N) exchange clusters. At the same time, for β-NiL$_2$, the exchange interactions for half of the (Ni^{2+}–O$^•$–N) clusters were proposed to be ferromagnetic. This assumption made us perform a detailed quantum-chemical investigation of exchange interaction mechanisms for α-NiL$_2$ and β-NiL$_2$.

Figure 8 shows schematically the relative position of the atoms of the chelating moiety and the coordinated N$^•$–O groups in the α-NiL$_2$ (a) and β-NiL$_2$ (b) complexes. The scheme was constructed on the basis of X-ray data. The same figure exhibits the magnetic orbitals of the complexes. As can be seen from Figure 8, the relative orientation of the paramagnetic Ni^{2+}-containing fragments of NiL$_2$ (below and in the figure denoted as $\{Ni^{2+}\}$) and coordinated fragments of adjacent molecules involving the N$^•$–O groups (below and in the figure denoted as $\{L_p\}$, $p = 1$ or 2) is determined by the geometrical parameters R, θ, φ, γ, and α. The values of these parameters for α-NiL$_2$ and β-NiL$_2$ are listed in Table 5.

---

(38) Porter, L. C.; Dickman, M. H.; Doedens, R. J. *Inorg. Chem.* **1988**, *27*, 1548.

(39) Caneschi, A.; Gatteschi, D.; Renard, J.-P.; Rey, P.; Sessoli, R. *Inorg. Chem.* **1989**, *28*, 2940.

(40) Caneschi, A.; Gatteschi, D.; Langier, J.; Rey, P.; Sessoli, R. *Inorg. Chem.* **1988**, *27*, 1553.

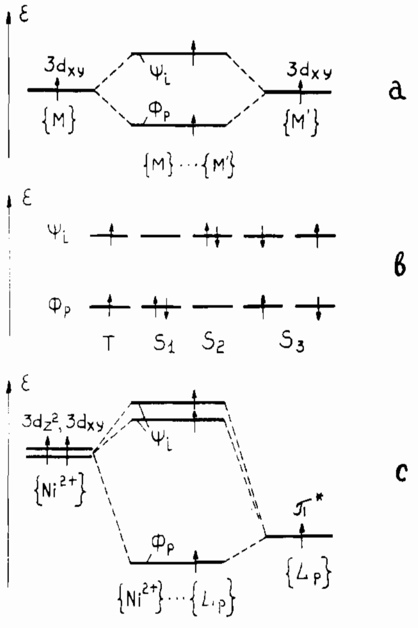

Figure 9. (a, c) Qualitative molecular orbital diagram of the interaction between magnetic orbitals for symmetrical (a) and nonsymmetrical (c) exchange systems. (b) Possible many-electron configurations in the frontier orbital basis.

Table 5. Geometrical Parameters of α-NiL$_2$ and β-NiL$_2$, Used in the Quantum-Chemical Calculations

compd	R, Å	θ, deg	φ, deg	γ, deg	α, deg
α-NiL$_2$	2.206	22.8	97.0	40.2	6.0
β-NiL$_2$	2.486	26.3	210.0	59.0	3.2
	2.302	25.8	30.0	5.4	4.2

The electronic structure of the heterospin exchange systems $\{Ni^{2+}\}\cdots\{L_p\}$ and $\{L_2\}\cdots\{Ni^{2+}\}\cdots\{L_1\}$ was calculated in terms of the INDO RHF (restricted Hartree–Fock) approach.[41] A schematic energy level diagram of unpaired electrons (frontier MO's) for the simplest model $\{Ni^{2+}\}\cdots\{L_p\}$ of the complexes under consideration is shown in Figure 9. An analysis of spin density distribution in the α-NiL$_2$ and β-NiL$_2$ has shown that in such complexes both unpaired electrons of the $\{Ni^{2+}\}$ fragment are mainly located on the 3d atomic orbitals ($\rho_{Ni}(1) = 0.89$, $\rho_{Ni}(2) = 0.81$) with a small delocalization toward the chelate group atoms and $\{L_1\}$ and $\{L_2\}$ radicals. Here $\rho_{Ni}(i)$ is the total spin density of an ith unpaired electron on the 3d AO's of Ni^{2+}. This allows one in good approximation to represent the ψ_i (i = 1, 2) MO's of these unpaired electrons as the sum

$$\psi_i = \varphi_i + \varphi_i^{del}$$

where $\varphi_i \simeq \sum_\mu c_{i\mu} f_\mu$, $f_\mu \equiv 3d_\mu$ AO ($\mu = z^2, xy, xz, yz, x^2 - y^2$) of Ni^{2+}; $\varphi_i^{del} \simeq \varphi_i^{L1} + \varphi_i^{L2}$ are the delocalization parts of MO's, involving the contributions of 2s and 2p AO's of the O$^\bullet$–N groups of $\{L_p\}$. Moreover, in the case of α-NiL$_2$ complexes, the φ_i parts of MO's can be well approximated by individual AO's

$$\varphi_1 \simeq 3d_{z^2}\ (\rho_{z^2}(1) = 0.86, \rho_{xy}(1) = 0.01)$$

$$\varphi_2 \simeq 3d_{xy}\ (\rho_{z^2}(2) = 0.02, \rho_{xy}(2) = 0.79)$$

while in β-NiL$_2$ complexes φ_i can be expressed in the form of linear combinations of these AO's

$$\varphi_1 \simeq c_1 3d_{z^2} + c_2 3d_{xy}\ (\rho_{z^2}(1) = 0.73, \rho_{xy}(1) = 0.16)$$

$$\varphi_2 \simeq c'_1 3d_{z^2} + c'_2 3d_{xy}\ (\rho_{z^2}(2) = 0.15, \rho_{xy}(2) = 0.68)$$

When the small delocalization in the direction $\{Ni^{2+}\} \rightarrow \{L_1\}, \{L_2\}$ ($\rho_{L_1}(i) + \rho_{L_2}(i) \leq 0.06$) is neglected, the MO's of the unpaired electrons of $\{Ni^{2+}\}$ have the simplest form $\psi_i \simeq \varphi_i$ ($\varphi_i^{del} = 0$). The unpaired electrons of the $\{L_p\}$ radicals are mainly localized on the π^*-antibonding MO's of the O$^\bullet$–N groups ($\rho_{L_p}(p) = 0.91$ for α-NiL$_2$, $\rho_{L_p}(p) = 0.89$ for β-NiL$_2$). The χ_p (p = 1, 2) MO's of these unpaired electrons can also be represented as the sum

$$\phi_p = \chi_p + \chi_p^{del}$$

where $\chi_p \simeq \pi^*$ MO's of the $\{L_p\}$ radicals; $\chi_p^{del} \simeq \chi_p^{Ni} + \chi_p^{L_{p'}}$ are the delocalization parts of MO's, including contributions from both the 3d AO's of Ni^{2+} and the 2s and 2p AO's of the O$^\bullet$–N group of the second radical $\{L_{p'}\}$ ($p' \neq p$). The smallness of the $\{L_p\} \rightarrow \{Ni^{2+}\}, \{L_{p'}\}$ delocalization ($\rho_{Ni}(p) + \rho_{L_{p'}}(p) \leq 0.04$) is also indicative of the possibility of the simple approximation of MO's $\phi_p \simeq \chi_p$ ($\chi_p^{del} = 0$).

It should be noted that the essentially localized type of MO's of unpaired electrons in the α-NiL$_2$ and β-NiL$_2$ complexes allows one to use the φ_i and χ_p orbitals as magnetic orbitals of the $\{Ni^{2+}\}$ and $\{L_p\}$ paramagnetic subsystems, e.g., in the analysis of direct exchange interactions. The role of spin density delocalization in the exchange interaction in such complexes will receive below a special consideration.

Direct Exchange Interaction. To elucidate the role of direct exchange interaction in the formation of the magnetic properties of α-NiL$_2$ and β-NiL$_2$ complexes, we performed calculations of the exchange parameters J for heterospin exchange systems $\{Ni^{2+}\}\cdots\{L_p\}$ (p = 1 or 2), taking into account the interaction only between unpaired electrons. The following expression was used:[26]

$$J = (1/n_A n_B)\sum_i^{n_A} J(i,p) \tag{3}$$

where

$$J(i,p) = \langle ip|pi\rangle - 2S_{ip}T_{pi} + S_{ip}{}^2[\epsilon_i + \epsilon_p - \langle p|U_A|p\rangle - \langle i|U_B|i\rangle + \langle ii|pp\rangle] \tag{4}$$

is the contribution to exchange interaction from the two MO's, $i \equiv \varphi_i$ and $p \equiv \chi_p$, belonging to the subsystems A $\equiv \{Ni^{2+}\}$ and B $\equiv \{L_p\}$. Here $n_A = 2$ and ϵ_i ($n_B = 1$ and ϵ_p) are, respectively, the number of unpaired electrons and orbital energies of the subsystem A (B); $S_{ip} = \langle i|p\rangle$ is the overlap integral between the φ_i and χ_p MO's; $T_{pi} = \langle p|\hat{T}|i\rangle$, where $\hat{T}$ is the kinetic energy operator; U_A (U_B) is the electrostatic potential formed by the core and the electronic shells of the subsystem A (B); $\langle ip|pi\rangle$ and $\langle ii|pp\rangle$ are the two-electron exchange and Coulomb integrals, respectively. The above INDO RHF MO's φ_i and χ_p localized on the Ni^{2+} ion and on the O$^\bullet$–N group, respectively, were taken as magnetic orbitals of interacting subsystems. All molecular integrals involved in $J(i,p)$ were calculated nonempirically using the familiar Gaussian basis sets.[42-44]

Earlier, when studying Cu^{2+}–nitroxide complexes, we established[45] that in the compounds involving the axial bonds Cu^{2+}–O$^\bullet$–N, the calculated exchange parameters $J(i,p) \simeq \langle 3d_{xy}\pi^*|\pi^* 3d_{xy}\rangle$ are positive due to the extremely small value of overlap $S_{ip} \leq 10^{-3}$ between the $\varphi_i \simeq 3d_{xy}$ AO and $\chi_p \simeq \pi^*$ MO of the $\{Cu^{2+}\}$

---

(41) Danovich, D. K.; Plakhutin, B. N. Information Materials of the Special Foundation for Quantum-Chemical Programs (Program N57). *Sib. Otd. Akad. Nauk SSSR* **1989**, *3*, 24.

(42) Basch, H.; Hornback, C. J.; Moskowitz, J. W. *J. Chem. Phys.* **1969**, *51*, 1311.

(43) Stewart, R. F. *J. Chem. Phys.* **1969**, *50*, 2485.

(44) Salez, C.; Veillard, A. *Theor. Chim. Acta* **1968**, *11*, 441.

(45) Musin, R. N.; Schastnev, P. V.; Malinovskaya, S. A. *Inorg. Chem.* **1992**, *31*, 4118.

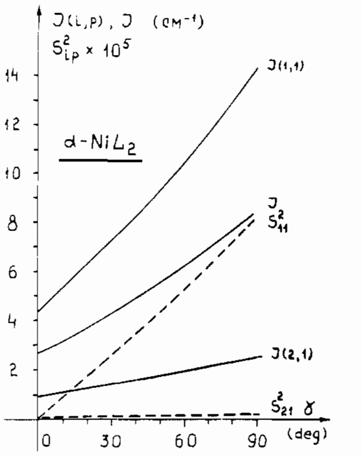

Figure 10. Variation of the values of the direct exchange parameters $J(i,p)$, J (solid lines) and the squared overlap integral between magnetic orbitals φ_i and χ_p, S_{ip}^2 (dashed lines), with γ for the exchange system $\{Ni^{2+}\}\cdots\{L_1\}$ of α-NiL₂.

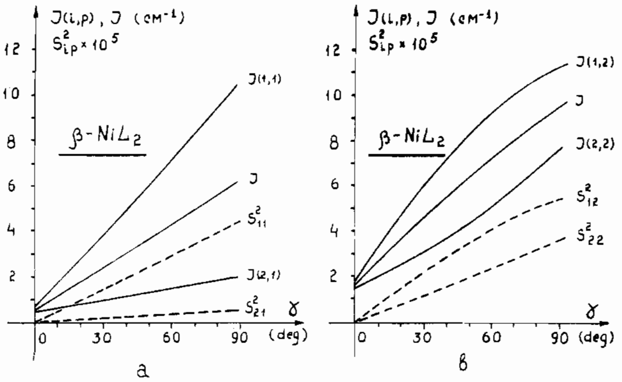

Figure 11. Variation of the values of the direct exchange parameters $J(i,p)$, J (solid lines), and the squared overlap integral between magnetic orbitals φ_i and χ_p, S_{ip}^2 (dashed lines) with γ for the exchange systems $\{Ni^{2+}\}\cdots\{L_1\}$ (a) and $\{Ni^{2+}\}\cdots\{L_2\}$ (b) of β-NiL₂.

and $\{L_p\}$ subsystems (the contribution of the terms proportional to S_{ip}^2 is negligible), but are approximately an order of magnitude less than the experimental ferromagnetic interaction values. At the same time, the strong antiferromagnetism of the complexes with equatorial Cu^{2+}–O•–N bonds can be well accounted for in terms of direct exchange mechanism since the favorable orientation of the magnetic orbitals φ_i and χ_p, in this case, significantly enlarges the overlap value $S_{ip} \simeq 0.1$, which results in large negative $J(i,p)$ values (the contribution of the terms proportional to S_{ip}^2 predominates). At first glance it would seem that this is also the case for the α-NiL₂ and β-NiL₂ complexes since for the compounds of this type the exchange parameter J should involve two similar contributions $J(i,p)$ (i = 1, 2) whose relative values and signs depend on the type of Ni^{2+}–O•–N coordination and on the efficiency of the overlap S_{ip} between the φ_i and χ_p MO's. Thus, for example, one could assume that the antiferromagnetic character of interactions in α-NiL₂ (J_{exp} = –69.4 cm⁻¹) is readily accounted for by the fact that the more effective overlap of the $\chi_p \simeq \pi^*$ MO of $\{L_p\}$ with the $\varphi_1 \simeq 3d_{z^2}$ AO (as compared with the overlap with the $\varphi_2 \simeq 3d_{xy}$ AO) of Ni^{2+} can lead to rather a significant negative contribution from $J(3d_{z^2},\pi^*)$, which would be higher in magnitude than the small positive contribution from $J(3d_{xy},\pi^*)$. However, our calculations invalidate this assumption. Figures 10 and 11 show plots for S_{ip}^2, $J(i,p)$ (i = 1, 2; p = 1 or 2) and J values versus the angle γ of $\{L_p\}$ rotation about the O(L_p)–N(L_p) bond, calculated (using expression 3 and 4) for the exchange systems $\{Ni^{2+}\}\cdots\{L_p\}$ of the α-NiL₂ and β-NiL₂ complexes at constant values of the other geometrical parameters R, θ, φ, and α (Table 5). As can be seen from these figures, even for the most favorable orientation (γ = 90°) of the magnetic orbitals φ_i and χ_p, the square of the overlap integral S_{ip}^2 does not exceed 10^{-4}. This is the reason for the positive contributions from MO pairs $J(i,p) \simeq \langle ip|pi\rangle$ for both α-NiL₂ and β-NiL₂. The J values approximately linearly increase with γ and are at a maximum at γ = 90°. The highest J values are no more than 10 cm⁻¹. It is also seen from Figures 10 and 11 that the exchange parameters J calculated for experimental γ angles (Table 5) are essentially different from experimental J_{exp}. For example, for α-NiL₂, J = 4.9 cm⁻¹ (J_{exp} = –69.4 cm⁻¹), and for β-NiL₂, J = 4.2 cm⁻¹ at p = 1 and 2.2 cm⁻¹ at p = 2 (J_{exp} = –115.0 and 9.8 cm⁻¹). Thus, it is shown that the observed magnetic properties of the α-NiL₂ and β-NiL₂ complexes cannot be accounted for in terms of a direct exchange mechanism.

Molecular Orbital Approach. Currently, the most widespread method for investigation of indirect exchange interactions with due account of the main molecular characteristics of the exchange system $\{A\}\cdots\{B\}$ (A and B are the paramagnetic subsystems) is the molecular orbital approach proposed by Hoffmann et al.[27] This approach is successfully applied to the interpretation of magnetic properties of bi- and polynuclear complexes of transition metals involving the symmetrical $\{M\}\cdots\{M'\}$ (or almost symmetrical) exchange systems with the same (or close) structures of magnetic orbitals and one-electron energy levels of the subsystems. At the same time, the legitimacy of applying this approach in studying exchange interactions in transition metal complexes with organic radicals, i.e., in the case of essentially nonsymmetrical exchange systems, such as $\{M\}\cdots\{L\}$, calls for a special check. Indeed, Hoffmann's approach was based on the consideration of singlet–triplet splitting in dimeric metal complexes (e.g., in the dimeric Cu^{2+} complexes) in terms of configuration interaction (CI) for frontier MO basis. Figure 9a,b shows a schematic diagram of one-electron molecular energy levels as well as many-electron configurations possible in such systems. An important characteristic feature of such symmetrical exchange systems is the fact that two frontier dimer MO's, $\psi_i \simeq \varphi^M - \chi^{M'}$ and $\phi_p \simeq \varphi^M + \chi^{M'}$ (φ^M, $\chi^{M'}$ = $3d_{xy}$ AO's of metal ions M and M′, if we use a cartesian axis system like that in Figure 8), have a different parity with respect to reflection (the C_{2v} symmetry). Hence, in determining the energy E^S_{min} of the lowest singlet state, one may restrict oneself to the consideration of the configuration interaction $\Psi^S = c_1S_1 + c_2S_2$ of only two singlet wave functions, $S_1 = |\phi_p\alpha\phi_p\beta K|$ and $S_2 = |\psi_i\alpha\psi_i\beta K|$, since the function $S_3 = 1/2^{1/2}\{|\phi_p\alpha\psi_i\beta K| - |\phi_p\beta\psi_i\alpha K|\}$ (K means inner closed-shell orbitals) will differ in parity from S_1 and S_2 and will not mix with them in the CI. Let the ψ_i and ϕ_p MO's be solutions of the Hartree-Fock equations for the high-spin (triplet) state $T = |\phi_p\alpha\psi_i\alpha K|$ with the energy E^T and the 2 × 2 CI matrix for the singlet states S_1 and S_2 be denoted by $\mathbf{R}$. Then, the result of solving the secular equation $|\tilde{\mathbf{R}} - \lambda\mathbf{I}| = 0$ for the transformed matrix

$$\tilde{\mathbf{R}} = \mathbf{R} - E^T\mathbf{I} = \begin{pmatrix} \Delta\epsilon + J_{pp} - J_{ip} + K_{ip} & K_{ip} \\ \cdots & -\Delta\epsilon + J_{ii} - J_{ip} + K_{ip} \end{pmatrix}$$

($\tilde{\mathbf{R}}$ is the symmetric matrix) yields directly the energies of singlet-triplet splittings $\lambda_n \equiv \Delta E_n^{ST} = E_n^S - E^T$ (n = 1, 2), and, hence, the exchange parameter (setting $E_k^S = E^S_{min}$ at $n = k$)

$$2J = \Delta E_k^{ST} = -J_{ip} + K_{ip} + {}^1/_2(J_{ii} + J_{pp}) - {}^1/_2\{[2\Delta\epsilon + (J_{ii} - J_{pp})]^2 + 4K_{ip}{}^2\}^{1/2} \quad (5)$$

which, on going to the basis of localized MO's, can be represented as the sum of ferromagnetic J_F and antiferromagnetic J_{AF} contributions:[27]

$$J = J_F + J_{AF} \quad (6)$$

Table 6. Calculated Values for α-NiL_2 of the Singlet–Triplet Splitting Energies $\Delta E_n^{ST}(i,p)$ (n = 1, 2, 3) for All Possible Pairs (i,p) of Unpaired Electrons (Frontier MO's ψ_i and ϕ_p) and the Exchange Parameters J (Using (7))

		MO		singlet–triplet splittings, cm^{-1}			param, cm^{-1}	
	approach	i	p	$\Delta E_1^{ST}(i,p)$	$\Delta E_2^{ST}(i,p)$	$\Delta E_3^{ST}(i,p)$	J	J_{exp}
$\{L_1\}$ $\{Ni^{2+}]$	without CI	1	1	6307.2	179 090.9	2076.0	547.7	
		2		7483.0	155 035.4	114.8		
	2 × 2 CI	1	1	6300.9	179 097.2		3445.9	–69.4
		2		7482.8	155 035.5			
	3 × 3 CI	1	1	7898.6	180 302.3	–726.8	–153.6 (–0.9)^b	
		2		7483.6	155 037.1	112.5		

^{a} J_{exp} is the experimental exchange parameter. ^{b} J obtained for the case of complete neglect of the spin density delocalization.

Here **I** is the unit matrix; $J_{ii} = \langle ii|ii\rangle$, $J_{pp} = \langle pp|pp\rangle$, and $J_{ip} = \langle ii|pp\rangle$ are the two-electron Coulomb integrals, and $K_{ip} = \langle ip|pi\rangle$ is the two-electron exchange integral of the ψ_i and ϕ_p MO's; $\Delta\epsilon = \epsilon_i - \epsilon_p$ is the difference of orbital energies. In the case of the α-NiL_2 and β-NiL_2 complexes with heterospin (nonsymmetrical) exchange systems $\{Ni^{2+}\}\cdots\{L_p\}$ (Figure 9c), the situation is more complicated since the CI leads to the mixing of all three singlet configurations $\Psi^S = c_1S_1 + c_2S_2 + c_3S_3$ (Figure 9b), and for correct estimation of the energies of singlet states E_n^S (n = 1, 2, 3) one should diagonalize the 3 × 3 CI matrix. Let this matrix be denoted as **D**. It can easily be shown that the transformed (symmetric) matrix $\tilde{\mathbf{D}}$ of the secular equation $|\tilde{\mathbf{D}} - \lambda\mathbf{I}| = 0$ for determining the singlet–triplet splittings $\lambda_n \equiv \Delta E_n^{ST}$ is given by[46]

$$\tilde{\mathbf{D}} = \mathbf{D} - E^T\mathbf{I} = \left[\begin{array}{c|c} \tilde{\mathbf{R}} & \begin{array}{c}\sqrt{2}G_{ip}\\ \sqrt{2}G_{pi}\end{array} \\ \hline \cdots\cdots & 2K_{ip} \end{array}\right]$$

Here $\tilde{\mathbf{R}}$ is the submatrix equivalent to the above 2 × 2 CI matrix of singlet–triplet splittings; $G_{ip} = \langle ip|pp\rangle$ and $G_{pi} = \langle pi|ii\rangle$ are the two-electron "hybrid" integrals of the ψ_i and ϕ_p MO's. The value of the exchange interaction in this case will be determined from the expression $2J = \Delta E_k^{ST} = E_k^S - E^T$ ($E_k^S = E_{min}^S$), as above. In general case of the exchange systems of the type $\{A\}\cdots\{B\}$, involving more than one unpaired electrons in the subsystems $\{A\}$ ($n_A \geq 1$) and $\{B\}$ ($n_B \geq 1$), for each pair of ψ_i (i = 1, ..., n_A) and ϕ_p (p = 1, ..., n_B) MO's the corresponding $\tilde{\mathbf{D}}$ matrix with the eigenvalues $\lambda_n = \Delta E_n^{ST}(i,p)$ can be determined. The exchange parameter J of such systems in a good approximation may be represented as a sum of $J(i,p) = {}^1/_2\Delta E_k^{ST}(i,p)$ contributions from the pairs of ψ_i and ϕ_p MO's:

$$J = (1/n_An_B)\cdot\sum_i^{n_A}\sum_p^{n_B} J(i,p) \qquad (7)$$

It should be noted that on studying exchange interactions in terms of molecular orbital approach it was usually assumed[47,48] that, in any case, the S_3 configuration corresponds to the excited electronic state (much higher in energy than the S_1 and S_2 states) and taking it into account in CI would yield only unessential corrections in the values of singlet–triplet splittings in exchange systems. Hence, as a rule, the contribution of the S_3 configuration to the singlet state wave function Ψ^S was neglected, and the exchange interactions in nonsymmetrical exchange systems were analyzed in terms of 2 × 2 CI, i.e., using expressions 5 and 6.

An important characteristic feature of the Ni^{2+} complexes with nitroxides is that the frontier MO's in such compounds are practically completely localized either on the O•–N group of the radical ($\phi_p \simeq \pi^*$ MO), or on the Ni^{2+} ion ($\psi_i \simeq$ 3d AO's). This means that the S_1 and S_2 configurations (Figure 9b) determine the excited singlet states $\Psi_1^S(E_1^S)$ and $\Psi_2^S(E_2^S)$ since for S_1 (doubly occupied ϕ_p MO), as well as for S_2 (doubly occupied ψ_i MO), the considered pair of magnetic electrons of the exchange system $\{Ni^{2+}\}\cdots\{L_p\}$ is localized in a narrow spatial region: either on the O•–N group or on the metal ion. In this case, a strong Coulomb repulsion occurs between the electrons of this pair, which results in destabilization of these singlet states. (It is well-known that the ion structures like (Ni^{3+}—O$^-$—N) or (Ni^+—O=$^+$N), arising in the complete electron transfer from the Ni^{2+} ion to the O•–N group or from the N•–O group to Ni^{2+}, respectively, cannot appear in the complexes under consideration because the Ni^{3+} and the oxammonium derivatives are too strong oxidants for such strong reducers as the hydroxylamine anion and Ni^+, respectively.) In fact, the Ni^{2+}–O•–N fragments correspond to the S_3 configuration with singly occupied ψ_i and ϕ_p MO's. It is precisely this configuration describing a spatially separated pair of magnetic electrons (with a weak Coulomb repulsion between them) that determines the lowest singlet state $\Psi_3^S(E_3^S)$ with the energy $E_3^S = E_{min}^S$. Since the triplet state electrons ($\Psi^T(E^T) \equiv T$) are also spatially separated, from simple qualitative considerations it is clear that the following order of energy levels should be typical of the heterospin exchange systems under investigation:

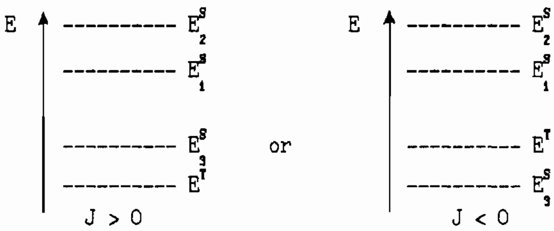

To support the validity of the above assumptions, for the simplest model $\{Ni^{2+}\}\cdots\{L_p\}$ of the α-NiL_2 and β-NiL_2 complexes with the INDO RHF MO's $\psi_i = \varphi_i + \varphi_i^{del}$ and $\phi_p = \chi_p + \chi_p^{del}$, we calculated the singlet–triplet splittings $\Delta E_n^{ST}(i,p)$ (n = 1, 2, 3) for all possible pairs (i, p) of unpaired electrons (the frontier MO's ψ_i and ϕ_p) as well as the exchange parameters J (by expression 7) in terms of three different approximations: (i) disregarding the CI (only the diagonal elements of the $\tilde{\mathbf{D}}$ matrix are considered), (ii) taking into account the 2 × 2 CI (diagonalization of the submatrix $\tilde{\mathbf{R}}$ of the $\tilde{\mathbf{D}}$ matrix), and (iii) taking into account the 3 × 3 CI ($\tilde{\mathbf{D}}$ matrix diagonalization). All needed matrix elements were calculated nonempirically using the Gaussian basis sets.[42–44] Calculated values of $\Delta E_1^{ST}(i,p)$ and J (as well as the experimental exchange parameters J_{exp}) are listed in Tables 6 and 7 for α-NiL_2 and β-NiL_2, respectively. Analysis of the singlet–triplet splitting energies $\Delta E_n^{ST}(i,p)$ shows that the singlet states $\Psi_1^S(E_1^S)$ and $\Psi_2^S(E_2^S)$, wherein the contributions from the S_1 and S_2 configurations, respectively, are predominant, do correspond to the high-excited energy states. Moreover, the calculated ΔE_1^{ST}(i,p) and $\Delta E_2^{ST}(i,p)$ splittings are weakly dependent on the type of

---

[46] Schastnev, P. V. Private communication.
[47] Van Kalkeren, G.; Schmidt, W. W.; Block, R. *Physica* **1979**, *97B*, 315.
[48] Hatfield, W. E. *Inorg. Chem.* **1983**, *22*, 833.

Table 7. Calculated Values for β-NiL_2 of the Singlet–Triplet Splitting Energies $\Delta E_n^{ST}(i,p)$ (n = 1, 2, 3) for All Possible Pairs (i, p) of Unpaired Electrons (Frontier MO's ψ_i and ϕ_p) and the Exchange Parameters J (Using (7))

		MO		singlet–triplet splittings, cm^{-1}			paramet, cm^{-1}	
	approach	i	p	$\Delta E_1^{ST}(ip)$	$\Delta E_2^{ST}(i,p)$	$\Delta E_3^{ST}(i,p)$	J	J_{exp}[a]
$\{L_1\}\cdots\{Ni^{2+}\}$	without CI	1 2	1	12 286.0 11 123.2	177 448.7 160 138.3	1831.3 1412.7	811.0	
	2 × 2 CI	1 2	1	12 280.9 11 119.9	177 454.1 160 142.4		5850.2	−115.0
	3 × 3 CI	1 2	1	13 328.8 12 806.1	178 554.2 160 752.2	−317.8 −884.0	−300.5 (0.5)[b]	
$\{Ni^{2+}\}\cdots\{L_2\}$	without CI	1 2	1	8 697.8 7 486.9	178 497.4 161 234.5	531.2 674.8	301.5	
	2 × 2 CI	1 2	1	8 697.4 7486.2	178 498.3 161 235.1		4045.9	9.8
	3 × 3 CI	1 2	1	8 772.5 7 724.9	178 793.8 161 570.0	160.1 100.3	65.1 (1.4)[b]	

[a] J_{exp} is the experimental exchange parameter. [b] J obtained for the case of complete neglect of the spin density delocalization.

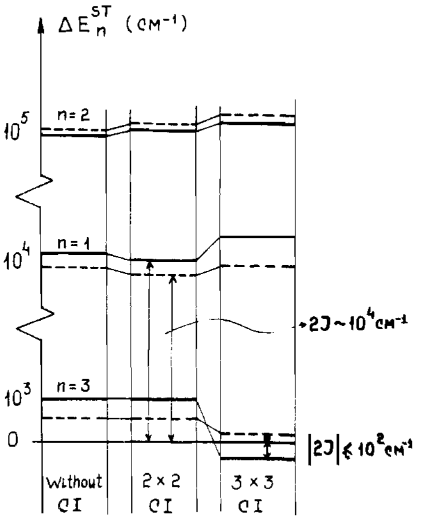

Figure 12. Schematic diagram of the averaged (by eq 8) singlet–triplet splitting energies ΔE_n^{ST} (n = 1, 2, 3) calculated for the exchange systems $\{Ni^{2+}\}\cdots\{L_1\}$ (solid lines) and $\{Ni^{2+}\}\cdots\{L_2\}$ (dashed lines) of β-NiL_2. Note the broken energy scale.

approximation used. In other words, in terms of the 3 × 3 CI approach, the admixture of the S_3 configuration practically has no effect on the position of these high-excited singlet energy levels E_1^S and E_2^S. At the same time, the 3 × 3 CI analysis allows one to reveal the low-lying singlet energy level (absent in the 2 × 2 CI approach) E_3^S with a wavefunction $\Psi_3^S(E_3^S)$ which is contributed mainly by the S_3 configuration. Obviously, it is the position of the lowest singlet energy level E_3^S (not E_1^S as it is assumed in terms of the 2 × 2 CI approach) that defines the value of exchange interaction parameter $J(i,p) = {}^1/_2\Delta E_3^{ST}(i,p)$ for a pair of unpaired electrons. For illustration, Figure 12 shows a schematic diagram of averaged singlet–triplet splitting energies

$$\Delta E_n^{ST} = {}^1/_2\sum_{i=1}^{2}\Delta E_n^{ST}(i,p) \qquad (8)$$

for two structurally different exchange systems $\{Ni^{2+}\}\cdots\{L_p\}$ (solid line for p = 1 and dashed line for p = 2) of the β-NiL_2 complex (see Figure 8). As can be seen, only the 3 × 3 CI analysis of singlet–triplet splittings allows one to establish the presence of both antiferromagnetic ($J < 0$) and ferromagnetic ($J > 0$) exchange interactions in the β-NiL_2 complex, which is consistent with magnetic measurements. It can be seen from Tables 6 and 7 that all J values calculated in this work for α-NiL_2 and β-NiL_2 coincide with the experimental parameters J_{exp} in sign and, moreover, they are close to J_{exp} in order of magnitude. Parenthetical values in these tables are the J values calculated (by expression 7) for the case of complete neglect of the spin density delocalization effects in the exchange systems $\{Ni^{2+}\}\cdots\{L_p\}$, i.e., at $\psi_i = \varphi_i$ ($\varphi_i^{del} = 0$) and $\phi_p = \chi_p$ ($\chi_p^{del} = 0$). The calculated J values are seen to be essentially different from experimental ones (J_{exp}). A detailed analysis of these results has shown that the J value is mainly formed by the contributions due to the small delocalization of unpaired electron density in the directions $Ni^{2+} \rightarrow O^{\bullet}$–N and $Ni^{2+} \leftarrow O^{\bullet}$–N, which leads to rather strong interactions (both exchange and Coulomb ones) in the Ni^{2+} and $O^{\bullet}$–N group of the radical. This allows one to make the conclusion that the main mechanism of exchange interaction in the considered complexes is the delocalization mechanism.

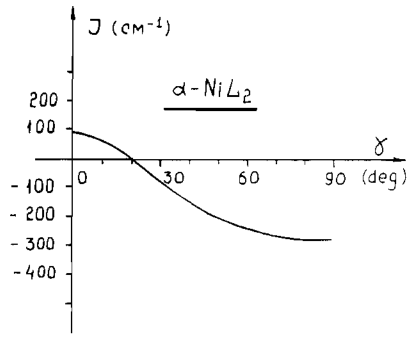

Figure 13. Variation of the exchange parameter J values, obtained in terms of the 3 × 3 CI approach, with γ for the exchange system $\{Ni^{2+}\}\cdots\{L_1\}$ of α-NiL_2.

To elucidate the question of what geometrical characteristics should be exhibited by the exchange system $\{Ni^{2+}\}\cdots\{L_p\}$ for ferromagnetic interactions to be realized, we (as in the case of direct exchange interactions) calculated the values of exchange parameters J (using expression 7) as functions of the angle γ of nitroxide $\{L_p\}$ rotation about the O–N bond at constant geometrical parameters R, θ, φ, and α (Table 5). The calculation results presented in Figures 13 and 14 show that a change in nitroxide orientation with respect to the chelate rings can result in altering both the value and the sign of the exchange parameter J. This is indicative of the fact that ferromagnetic exchange interactions can occur not only in β-NiL_2 complexes, but even in α-NiL_2 complexes, i.e., in the Ni^{2+} complexes with axially coordinated $O^{\bullet}$–N groups of nitroxides in the case of small γ angles (≤20°) at which the φ_i and χ_p magnetic orbitals of the $\{Ni^{2+}\}$ and $\{L_p\}$ subsystems are almost orthogonal.

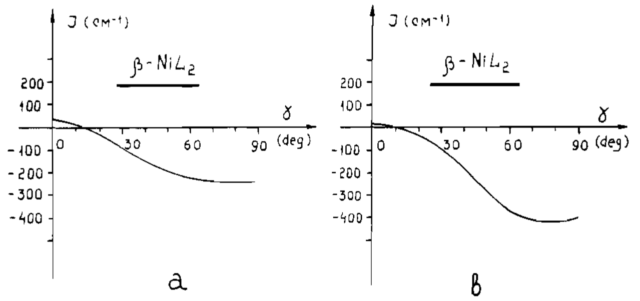

Figure 14. Variation of the exchange parameter J values, obtained in terms of the 3 × 3 CI approach, with γ for the exchange systems $\{Ni^{2+}\}\cdots\{L_1\}$ (solid line) and $\{Ni^{2+}\}\cdots\{L_2\}$ (dashed line) of β-NiL_2.

It should be noted in conclusion that the characteristic features of exchange interactions in the Ni^{2+}–nitroxide complexes, considered in this work, should be the case, in general, for heterospin complexes involving the (M^{n+}–O•–N) exchange clusters.

Conclusion

1. The unusual magnetic properties of NiL_2, mentioned in the Introduction, are determined by the nature of the complex able to exist in two polymorphs.

2. The results of our investigation show that the polymorphous modifications α-NiL_2 and β-NiL_2 exhibit essentially different magnetic properties. Hence, the ability of the nitroxide-containing complex to exist in a few polymorphous modifications calls for a special check of the polymorphous homogeneity of tested polycrystalline samples.

3. Of particular interest is the unusual fact of ferromagnetic exchange in β-NiL_2 in the presence of direct contact of nonorthogonal magnetic orbitals. The probability of ferromagnetic exchange interactions in (Ni^{2+}–O•–N) exchange clusters, as shown in this work, is rather high. This might be useful in design of molecular ferromagnets based on Ni^{2+} complexes with stable nitroxides (as the ferromagnetic exchange provides the highest values of spontaneous magnetization for compounds able to undergo the magnetic phase transition to the ferromagnetic state).

4. The polymeric layer structure in α-NiL_2 is practically the same as that in previously studied $NiL_2(ROH)_2$. The only difference is that in solid $NiL_2(ROH)_2$ (see the scheme in Introduction), unlike in α-NiL_2, the O–H groups of coordinated alcohol molecules are situated between Ni^{2+} ions and O•–N groups of adjacent molecules. This essentially weakens the antiferromagnetic exchange interaction between unpaired electrons of Ni^{2+} and O•–N groups and leads to larger residual spins of the exchange clusters as compared to the residual spins of the (N•–O–Ni^{2+}–O•–N) clusters, which is enough for the magnetic phase transition to the ferromagnetic state $NiL_2(ROH)_2$ to be realized at 5–7 K. The stronger antiferromagnetic exchange in α-NiL_2 results in a dramatic decrease of residual spin of the exchange cluster (N•–O–Ni^{2+}–O•–N) with temperature decrease, which is unfavorable for the realization of the magnetic phase transition in this modification of the complex.

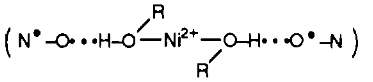

$$(N^{\bullet}{-}O\cdots H{-}O(R){-}Ni^{2+}{-}O(R){-}H\cdots O^{\bullet}{-}N)$$

5. In quantum-chemical analysis of exchange interactions in the heterospin exchange clusters (M^{n+}–O•–N) with essentially localized unpaired electrons, the lowest singlet state energies (and, hence, the values of exchange parameters J) in the basis of frontier MO's ψ_i and ϕ_p can be estimated correctly in terms of the 3 × 3 CI including the singly excited configuration $1/2^{1/2}\{|\phi_p\alpha\psi_i\beta K| - |\phi_p\beta\psi_i\alpha K|\}$. The contributions due to the small delocalization of spin density from metal ion to the O•–N group and from the O•–N group to metal ion should also be taken into account.

6. It should be noted in addition that along with the NiL_2-type compounds, which can be obtained and studied as separate polymorphous modifications, there are metal complexes with nitroxides whose individual solids involve alternating molecules belonging to different conformations.[49–52] The analysis of the magnetic properties of such compounds is thus far an unresolved problem. We believe that further investigation of the complexes with radicals able to exist as various polymorphous modifications would allow one to approach the theoretical interpretation of the magnetic properties of the compounds whose crystals involve simultaneously the molecules belonging to different conformations.

Acknowledgment. This work was supported by the Russian Fundamental Research Foundation through Grants No. 93-03-5339 and No. 93-03-5023. We also thank Prof. P. V. Schastnev for the calculation of the magnetic susceptibility for β-NiL_2 in terms of the heterospin three-center exchange cluster model.[53]

Supplementary Material Available: Tables giving the structure determination summary, complete positional parameters, bond lengths and angles, and anisotropic thermal parameters for α-NiL_2 and β-NiL_2 (Tables S1–S8) (15 pages). Ordering information is given on any current masthead page.

---

(49) Anderson, O. P.; Kuechler, T. C. *Inorg. Chem.* **1980**, *19*, 1417–1422.

(50) Grand, A.; Rey, P.; Subra, R. *Inorg. Chem.* **1983**, *22*, 391.

(51) Gatteschi, D.; Langier, J.; Rey, P.; Zanchini, C. *Inorg. Chem.* **1987**, *26*, 938.

(52) Volodarsky, L. B.; Reznikov, V. A.; Ovcharenko, V. I. *Synthetic Chemistry of Stable Nitroxides*; CRC Press: Boca Raton, FL, Ann Arbor, MI, London, Tokyo, 1994.

(53) Malinovskaya, S. A.; Schastnev, P. V. *Zh. Strukt. Khim.* **1993**, *33*, N4, 66.